Testing Dissipative Collapse Models with a Levitated Micromagnet

A. Vinante,[1,2,*] G. Gasbarri,[1,†] C. Timberlake,[1] M. Toroš,[3] and H. Ulbricht[1,‡]

[1] *School of Physics and Astronomy, University of Southampton, SO17 1BJ, Southampton, UK*
[2] *Istituto di Fotonica e Nanotecnologie - CNR and Fondazione Bruno Kessler, I-38123 Povo, Trento, Italy*
[3] *Department of Physics and Astronomy, University College London, Gower Street, London WC1E 6BT, UK*

(Dated: August 17, 2020)

We present experimental tests of dissipative extensions of spontaneous wave function collapse models based on a levitated micromagnet with ultralow dissipation. The spherical micromagnet, with radius $R = 27\ \mu$m, is levitated by Meissner effect in a lead trap at 4.2 K and its motion is detected by a SQUID. We perform accurate ringdown measurements on the vertical translational mode with frequency 57 Hz, and infer the residual damping at vanishing pressure $\gamma/2\pi < 9\ \mu$Hz. From this upper limit we derive improved bounds on the dissipative versions of the CSL (continuous spontaneous localization) and the DP (Diósi-Penrose) models. In particular, dissipative models give rise to an intrinsic damping of an isolated system with the effect parameterized by a temperature constant – the dissipative CSL model with temperatures below 1 nK is ruled out, while the dissipative DP model is excluded for temperatures below 10^{-13} K. Furthermore, we present the first bounds on dissipative effects in a more recent model, which relates the wave function collapse to fluctuations of a generalized complex-valued spacetime metric.

Spontaneous wave function collapse models [1–6] are a well established approach in the context of quantum foundations. The key idea is that the unitary evolution of standard quantum mechanics must be modified by additional phenomenological terms in order to explain the emergence of definite and stochastic outcomes in measurement processes. These additional terms must be nonlinear and stochastic, leading to a fundamental breaking of the quantum superposition principle. In a nutshell, collapse models postulate the existence of some kind of classical noise field, the nature of which is either unknown [1, 2] or related to a cosmological or to the gravitational field [3, 4]. It has also been suggested that collapse models could be related to the long standing problem of the incompatibility between quantum mechanics and general relativity [7]. In this latter respect, other related phenomenological models have been recently investigated [8–11].

Collapse models are usually parameterized by only a few free parameters: a collapse rate which sets the strength of the collapse mechanism, and a localization length which quantifies the localization precision. The parameters of the model can be considered as independent, as in the continuous spontaneous localization (CSL) model [2], or fixed by theoretical considerations, e.g. the collapse rate in the Diósi-Penrose (DP) model which is set by gravity.

A well-known issue of collapse models is the energy divergence problem: the collapse noise feeds continuously energy into any material system, implying an unbounded rate of increase of energy in the universe [1]. This problem is solved by dissipative extensions of collapse models, in which the noise is associated to a dissipative mechanism and can thus be thought as a thermal bath interacting with ordinary matter [12, 13]. In this framework, the energy can flow in both directions and will not diverge with time anymore. Dissipative models imply the existence of a fundamental and universal damping mechanism which can be in principle probed by mechanical systems with very low dissipation [14].

In this paper we perform new experimental tests of the dissipative versions of the continuous spontaneous localization (CSL) model [12, 15] and the DP model [13, 14], also known as dCSL and dDP. Our experiment is based on a magnetically levitated microsphere with ultralow damping. In particular, our data exclude a new portion of the parameter space compared to previous experiments [14] substantially excluding collapse temperatures lower than 10^{-9} K for the dCSL model and 10^{-13} K for the dDP model. In addition, we test for the first time a more recent model first proposed by Adler [8, 16], which assumes the collapse noise to arise from complex fluctuations of the gravitational field, or equivalently of the spacetime metric. We refer to this model as CGF (complex gravity fluctuations). We show that our data allow to probe complex fluctuations of the metric with an imaginary part down to 10^{-22}.

I. THEORY

A. The dCSL model

CSL, the most studied among collapse models, is constructed in such way to produce a spatial localization of the wavefunction, i.e. a collapse in position. The localization rate scales with the mass of the system, implying a rapid collapse of the center-of-mass position of any macroscopic system, while giving no measurable effect at the microscopic level, where conventional quan-

*Electronic address: andrea.vinante@ifn.cnr.it
†Now at: Universitat Autònoma de Barcelona
‡Electronic address: h.ulbricht@soton.ac.uk

tum mechanics is recovered. The standard CSL model has two free parameters, the collapse rate conventionally referred to a single nucleon λ, and a characteristic length r_c. Many different experimental techniques have been recently proposed or implemented to test the CSL model. While true interferometric tests have recently achieved impressive sensitivity [17, 18], even more stringent bounds on the CSL collapse rate λ have been established by non-interferometric experiments looking at noise and diffusion in mechanical systems [19–24] or cold atoms [25], or in spontaneous generation of x-ray photons [26] or high frequency phonons [27].

The dCSL model has been explicitly introduced to remove the energy divergence of the standard CSL model [12]. Formally, in dCSL the collapse happens both in position and in momentum [12]. The evolution of the density matrix of the center-of-mass of a rigid body along a fixed direction x is described, in the limit of small x and p, by the following Lindblad-type master equation [15]:

$$\begin{aligned}\frac{\mathrm{d}\hat{\rho}}{\mathrm{d}t} =& -\frac{i}{\hbar}[\hat{H},\hat{\rho}] - \frac{\eta}{2}[\hat{x},[\hat{x},\hat{\rho}]] - \frac{\gamma_c^2}{8\eta\hbar^2}[\hat{p},[\hat{p},\hat{\rho}]] \\ &- \frac{i\gamma_c}{2\hbar}[\hat{x},\{\hat{p},\hat{\rho}\}],\end{aligned} \tag{1}$$

where $\hat{H}$ is the standard Hamiltonian, the second and third term on the right hand side describes position and momentum decoherence/diffusion due to the dCSL effect and the fourth one accounts for dCSL energy dissipation.

Under the assumption $r_c \gg a$ [28] with a interatomic distance, the diffusion parameter η can be expressed as a function of the free parameters of the model and the mass distribution of the rigid body [14, 15]:

$$\eta = \frac{(4\pi)^{\frac{3}{2}}\,\lambda\, r_c^3}{\hbar^2 m_0^2 (2\pi\hbar)^3}\int \mathrm{d}\mathbf{q}\,|\tilde{\varrho}(\mathbf{q})|^2\, e^{-\frac{\mathbf{q}^2 r_c^2(1+\chi)^2}{\hbar^3}}\, q_x^2 \tag{2}$$

with m_0 the nucleon mass, $\mathbf{q} = (q_x, q_y, q_z)$ the momentum, $\varrho(\mathbf{r})$ the mass density in the coordinate space and

$$\tilde{\varrho}(\mathbf{q}) = \int \mathrm{d}\mathbf{r}\, e^{\frac{i\mathbf{q}\cdot\mathbf{r}}{\hbar}}\, \varrho(\mathbf{r}) \tag{3}$$

its Fourier transform.

The free parameters of the model are the collapse rate λ, the characteristic length r_c, and the dimensionless dissipation parameter χ. The latter can be rewritten in terms of a new parameter T_c in the following way [14]:

$$\chi = \frac{\hbar^2}{8 m_a r_c^2 k_B T_c}. \tag{4}$$

T_c can be interpreted as the temperature of the collapse field [12]. The energy dissipation rate of the center-of-mass dynamics can be written as [12, 15]:

$$\gamma_c = 4\eta r_c^2 \chi\,(1+\chi)\,\frac{m_a}{m} \tag{5}$$

where m is the total mass and m_a is a reference mass for the elementary entity which constitutes the physical object. Following the convention in Ref. [14], we choose m_a to be the nuclear mass. With this choice we implicitly assume the internal dynamics of nuclei irrelevant for the CSL mechanism, assumption justified by r_c being much larger than the nuclear size.

As one may notice, the standard CSL is recovered when $\chi = 0$, that according to Eq. (4) corresponds to a CSL field with infinite temperature. Technically, this implies an energy divergence, as the CSL noise will continuously transfer energy to the system causing an unbounded momentum diffusion. This unpleasant consequence is removed in the dissipative version. Indeed, an isolated system will eventually thermalize to T_c [12], meaning that for temperatures higher than T_c the dCSL noise will effectively act as a refrigerator. The proponents of the dCSL model further propose that reasonable values for T_c should be around 1 K, by analogy to other known cosmological fields such as cosmic microwave photons or cosmic neutrinos [12]. Concerning the other parameters two main proposals are known in literature for the CSL model, the initial guess by Ghirardi *et al.* who proposed $\lambda \approx 10^{-16}$ Hz at $r_c = 10^{-7}$ m [1] and the one by Adler, who proposed a much higher value $\lambda \approx 10^{-8\pm2}$ Hz at $r_c = 10^{-7}$ m, motivated by making the collapse effective at mesoscopic scale [29].

For the case relevant to our work, namely a homogeneous sphere of radius R and density ϱ, the Fourier transform of the mass density is

$$\tilde{\varrho}(q) = \frac{3m\hbar}{qR} J_1(qR/\hbar), \tag{6}$$

where J_i represents the i-th spherical Bessel function. The integral in Eq. (2) can be analytically solved [14] providing the diffusion constant and dissipation rate:/

$$\eta = \frac{3\lambda m^2 r_c^2}{(1+\chi)\, m_0^2 R^4} K\left[\frac{R}{r_c\,(1+\chi)}\right], \tag{7}$$

$$\gamma_c = \frac{3\lambda\hbar^2 m m_a r_c^2}{2 k_B T_c m_0^2 R^4} K\left[\frac{R}{r_c\,(1+\chi)}\right], \tag{8}$$

where we have defined for convenience:

$$K(y) = 1 - \frac{2}{y^2} + e^{-y^2}\left(1 + \frac{2}{y^2}\right). \tag{9}$$

The function $K(y)$ can be approximated by 1 and $y^4/6$ for large and small y, respectively. This determines the behaviour of η and γ_c as function of r_c. In the limit of small dissipation $\chi \ll 1$ both functions are proportional to r_c^2 if $r_c \ll R$ and to r_c^{-2} if $r_c \gg R$, with a shallow maximum at $r_c \approx R$. This picture breaks down for very low T_c, such that $\chi > 1$. In this limit both diffusion and dissipation feature a stronger dependence on r_c for small r_c, corresponding to $\eta \propto r_c^8$ and $\gamma_c \propto r_c^6$, respectively.

B. The dDP model

The fact that the collapse localization rate scales with the mass of the system suggests a natural connection to gravity. The Diósi-Penrose (DP) model [3, 4] is an attempt to provide this link. Although proposed by Diósi [3], the model is known in literature as DP because it captures some features of a related proposal by Penrose [4]. The master equation of the DP model is almost identical to the one of CSL, only differing from the latter in the localization operator. However in the DP model the collapse strength is set proportional to the gravitational constant G rather than depending on a free parameter. As such, the standard DP model features only one free parameter, a regularization length R_0 [9]. Proposed values for R_0 range from 10^{-15} m [3] to 10^{-7} m [30].

A dissipative extension of the DP model (so called dDP model) can be developed in a similar way as the dCSL [13, 14]. One defines a dissipation parameter $\chi_{\rm DP}$, which can be rewritten in terms of a collapse field temperature $T_{\rm DP}$:

$$\chi_{\rm DP} = \frac{\hbar^2}{8 m_a R_0^2 k_B T_{\rm DP}}. \tag{10}$$

In the limit of uniform mass density in which the characteristic length $R_0' = R_0 \left(1 + \chi_{DP}\right)$ is larger than the interatomic distance a, the expression for the diffusion constant for a homogeneous sphere was calculated in [14] as:

$$\eta_{\rm DP} = \frac{G m^2}{\sqrt{\pi} R^3} I\left(\frac{R}{R_0'}\right) \tag{11}$$

where we have defined for convenience:

$$I(y) = \sqrt{\pi}\,\mathrm{Erf}(y) + \frac{1}{y}\left(e^{-y^2} - 3\right) + \frac{2}{y^3}\left(1 - e^{-y^2}\right). \tag{12}$$

The dissipation rate $\gamma_{\rm DP}$ is then calculated as:

$$\gamma_{\rm DP} = 4\eta R_0^2 \chi_{\rm DP}\left(1 + \chi_{\rm DP}\right)\frac{m_a}{m}. \tag{13}$$

The function $I(y)$ can be approximated by $y^3/6$ for $y \ll 1$ and tends to $\sqrt{\pi}$ for $y \gg 1$. Therefore, the collapse/diffusion parameter $\eta_{\rm DP}$ scales with m^2 for $R < R_0'$ and with m for $R > R_0'$. This behaviour is typical of collapse models, and can be interpreted as a coherent amplification of the collapse rate within a sphere of radius R_0' [31].

In the opposite limit, i.e. when $R_0 \ll a$ the assumption of homogeneity is no longer valid and we need to consider the granularity of the matter distribution. In this regime the diffusion parameter η_{DP} can be calculated by means of a lattice model and the following expression obtained:

$$\eta_{\rm DP} = \frac{G}{6\hbar\sqrt{\pi}(1 + \chi_{\rm DP})^3 R_0^3} m_a m, \tag{14}$$

The attentive reader can find detailed calculations in Appendix. We note that, in contrast with the CSL model, the granular limit for the DP model is often suggested because it allows to enhance the collapse rate, making it closer to experimental testability [9]. R_0 as low as the nuclear size has been proposed in literature – indeed the DP model is nonrelativistic and the nucleon scale is a natural limit for the nonrelativistic regime [9].

We note that in the dDP model there are only two free parameters, the regularization length R_0 and the collapse field temperature $T_{\rm DP}$. Similarly as in dCSL, a system will eventually thermalize to the temperature $T_{\rm DP}$, while for the standard DP model there is no dissipation, leading to an energy divergence.

C. The CGF model

The complex gravity fluctuations (CGF) model is based on assuming the existence of complex fluctuations of the gravitational field, or equivalently of the spacetime metric. The idea, first proposed by Adler [8] and further developed in Refs. [16] and [9], can be summarized as follows.

A gravitational field $h_{\mu\nu}$ couples to the stress energy tensor $T_{\mu\nu}$ of the system. In a linearized fully quantum theory [32] this implies the existence of a coupling term $H_{\rm int} = \frac{1}{2} h_{\mu\nu} T^{\mu\nu}$ in the Hamiltonian, that in the non relativistic regime can be simplified as $H_{\rm int} = \frac{1}{2} h_{00} m c^2$. This ultimately leads to a master equation of decoherence type such as Eq. (1). However, if one assumes that the metric remains classical, but involves rapidly fluctuating complex terms, the resulting classical noise field would feature an antihermitian coupling to matter [9, 16], which is the basic ingredient required to produce the collapse/localization of the wavefunction, as opposed to quantum decoherence. While in general relativity the metric is rigorously real-valued, complex effective metrics have been actually proposed in some modified gravity theories with chiral deformations [33].

The noise-matter coupling in the case of classical complex noise will also lead to the appearance of nonlinear terms in the master equation. The derivation of the appropriate master equation for the center of mass of mechanical oscillator is reported in Ref. [16]. Here, we rewrite Eq. (D5) in Ref. [16] as:

$$\begin{aligned}\partial_t \hat{\rho} = & \frac{i}{\hbar}[\hat{H}_0, \hat{\rho}] - \eta_{\rm CGF}\left[\hat{x}, [\hat{x}, \hat{\rho}]\right] + \frac{\gamma^{\rm R}_{\rm CGF}}{2\hbar}\left[\hat{x}, [\hat{p}, \hat{\rho}]\right] \\ & - i\frac{\gamma^{\rm I}_{\rm CGF}}{2\hbar}\left[\hat{x}, \{\hat{p}, \hat{\rho}\}\right]\end{aligned} \tag{15}$$

with $\hat{H}_0$ the Hamiltonian characterising the harmonic oscillator free dynamics, and

$$\eta_{\rm CGF} = \frac{c^4 \xi^2}{6\pi^2\hbar^7}\int_0^\infty dq \int d\tau\, D^{\rm R}(q,\tau)\tilde{\varrho}(q)^2 q^4 \tag{16}$$

$$\gamma^{\rm I/R}_{\rm CGF} = \frac{c^4 \xi^2}{3\pi^2\hbar^6 m}\int_0^\infty dq \int d\tau\, \tau D^{\rm I/R}(q,\tau)\tilde{\varrho}(q)^2 q^4 \tag{17}$$

where $D^{\rm I/R}(q,\tau)$ are the real and imaginary part of the normalized correlator of the complex metrics fluctuations, expressed as function of time τ and momentum

q, and ξ is the dimensionless magnitude of the correlator. The dissipative term, with energy dissipation rate $\gamma^{\rm I}_{\rm CGF}$, depends only on the imaginary part of the correlator, while the real part leads to diffusion. To proceed we assume that the imaginary part of correlator can be written as $D^{\rm I}(q,\tau) = f(\tau)d(q)$ with

$$\begin{aligned} f(\tau) &= e^{-\lambda\tau} \\ d(q) &= r_c^3\, e^{-r_c^2 q^2/\hbar^2} \end{aligned} \tag{18}$$

so to have $D(r,\tau)$ dimensionless and characterized by Gaussian spatial correlation with width r_c as in the CSL model, and a time correlation with single exponential parameter λ. By inserting the mass density Eq. (6) and carrying out the integration we obtain

$$\begin{aligned} &\int_0^\infty d\tau\, \tau e^{-\lambda\tau} = \lambda^{-2} \\ &\int_0^q q^4 d(q)|\tilde{\varrho}(q)|^2 = \frac{9r_c^2\hbar^5 m^2\sqrt{\pi}}{4R^4} K\left(\frac{R}{r_c}\right) \end{aligned} \tag{19}$$

and combining the results together in Eq. (17) we find:

$$\gamma^{\rm I}_{\rm CGF} = \frac{6r_c^2 c^2\xi^2}{(4\pi)^{\frac{3}{2}} R^4\lambda^2}\frac{mc^2}{\hbar} K\left(\frac{R}{r_c}\right). \tag{20}$$

Note that, due to the assumption of gaussian spatial correlation, Eq. (20) is very similar to the expression of γ_c in the dCSL case Eq. (8). If we further assume that temporal and spatial correlations are related to each other by the speed of light and set $\lambda = c/r_c$, we obtain:

$$\gamma^{\rm I}_{\rm CGF} = \frac{6mc^2\xi^2}{(4\pi)^{\frac{3}{2}}\hbar}\frac{r_c^4}{R^4} K\left(\frac{R}{r_c}\right). \tag{21}$$

This further assumption is suggested by the fact that the gravitational field propagates at speed of light [16].

II. EXPERIMENTAL SETUP

Experimentally, we follow the approach outlined in Ref. [14]. By preparing and measuring a mechanical resonator with very low friction it is possible to set an upper bound on the fundamental dissipation predicted by collapse models. The advantage of this approach is that measuring very low dissipation is experimentally less challenging than measuring noise. In fact, ultralow mechanical dissipation is more easily achieved at low frequencies, where excess vibrational noise of seismic or acoustic origin are ubiquitous and very hard to shield.

Our mechanical resonator is a translational mode of a ferromagnetic microsphere levitated and confined by Meissner effect in a superconducting trap. The experimental setup has been described in detail in Ref. [34]. The microsphere is made of a neodymium-based alloy with density $\varrho = 7.4\times10^3$ Kg/m^3 and radius $R =$ (27 ± 1) μm (Fig. 1), fully magnetized in a 10 T NMR magnet prior to the experiment, with an expected saturated magnetization $\mu_0 M \approx 0.7$ T. It is levitated by Meissner effect inside a cylindrical well machined in a 99.95%-purity Pb block with 4 mm diameter and 4 mm depth. The Meissner surface currents induced by the magnetic microsphere, combined with gravity, provide full confinement in all spatial direction. The motion of the microsphere is detected by a commercial dc SQUID connected through a single pick-up coil placed above the levitated particle. The pick-up coil consists of 6 loops of NbTi wire, wound around a cylindrical PVC holder with radius 1.5 mm, coaxial with the trap. The setup is mounted inside a magnetically shielded copper vacuum chamber filled with a variable pressure of helium gas, which is dipped in a standard helium transport dewar at $T = 4.2$ K. We monitor the helium pressure in the vacuum chamber with a Pirani-Penning gauge placed at room temperature. The actual pressure at the microsphere location is then estimated by applying a correction which takes into account the thermomolecular pressure drop [34, 35]. In the low pressure limit, this can be approximated as $P/P_0 = (T/T_0)^{\frac{1}{2}}$ where P and $T = 4.2$ K are pressure and temperature at the microsphere location, P_0 is the helium pressure measured by the gauge at room temperature and $T_0 \approx 300$ K.

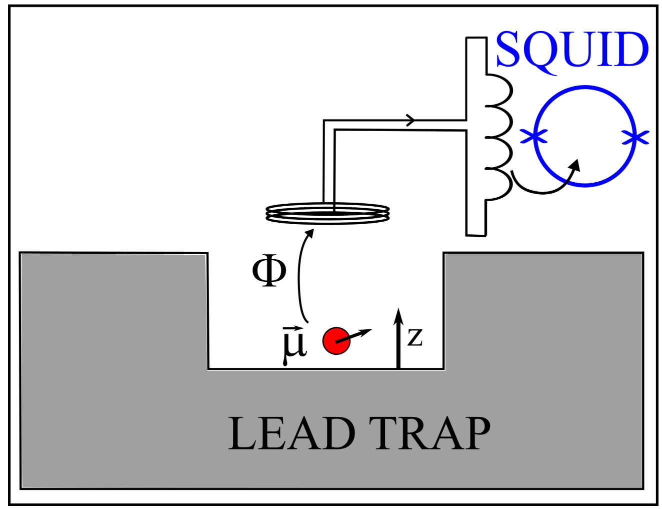

FIG. 1: Simplified scheme of the experimental setup. A micromagnetic sphere with permanent magnetic moment $\boldsymbol{\mu}$ is levitated by Meissner effect in a cylindrical well machined in a type-I superconductor (lead). The motion of the micromagnet is trapped in all degrees of freedom. For this work we consider specifically the vertical motion along z, which features a resonance frequency $f_0 = 56.8$ Hz. The motion is monitored by a commercial SQUID through the flux $\delta\Phi \propto \delta z$ induced in a superconducting pick-up coil.

As discussed in Ref. [34], the SQUID is able to detect 5 degrees of freedom of the rigid body. Comparison with a finite element simulation allows to reliably identify 3 translational modes and 2 librational modes. In this work we focus on the vertical translational mode, which we refer to as the $z-$mode. For this mode the resonance frequency can be also estimated by applying the image method to a magnetic dipole above an infinite plane [34]:

$$f_0 = \frac{1}{\pi}\sqrt{\frac{g}{z_0}} \tag{22}$$

where z_0 is the equilibrium height:

$$z_0 = \left(\frac{3\mu_0\mu^2}{64\pi mg}\right)^{\frac{1}{4}} \tag{23}$$

Here, $\mu = MV$ is the total magnetic dipole moment with M saturation magnetization and V volume, $m = \varrho V$ is the mass, and g is the gravity acceleration. For our microsphere we estimate $f_0 = 59.0$ Hz, not far from the measured value $f_0 = 56.8$ Hz.

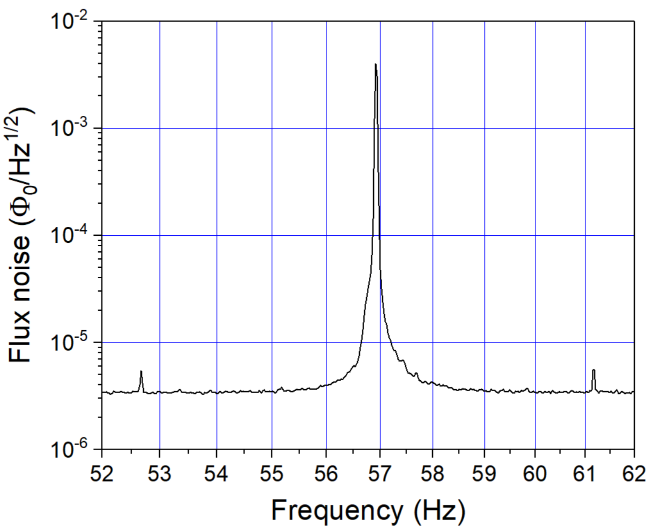

FIG. 2: Typical power spectrum of the $z-$mode over 12 hours, acquired at a pressure $P = 5.6 \times 10^{-5}$ mbar. The two small satelites correspond to a nonlinear mixing with an horizontal mode at 4.3 Hz

III. EXPERIMENTAL RESULTS

Fig. 2 shows an uncalibrated spectrum of the $z-$mode, expressed in units of voltage at the output of the SQUID electronics, and averaged over 12 hours. The resonance frequency is remarkably stable over time, featuring only small amplitude-dependent shifts due to anharmonicities in the trapping potential. During the measurements relevant to this paper these shifts are always smaller than 1 Hz.

Fig. 3 shows a ringdown measurement of the $z-$mode. The mode is excited by sending an ac current of the order of 1 mA through a single loop excitation coil wound on the pick-up coil holder. After excitation, we monitor the ringdown by means of a lock-in amplifier with reference frequency f_r set close to the actual amplitude dependent resonance frequency f_0. Before any amplitude measurement we precisely adjust f_r to f_0 to better than 1 mHz by nulling the phase drift rate. The error bar on each point is calculated by adding in quadrature the mean amplitude of the peak when it is dominated by noise. The data in

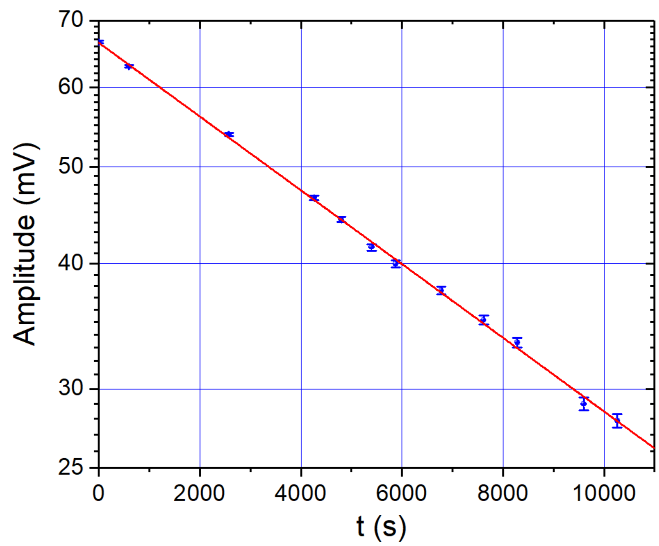

FIG. 3: Ringdown measurement performed at $P = 1.35 \times 10^{-5}$ mbar. The weighted exponential fit provides the amplitude decay time $\tau = (1.19 \pm 0.01) \times 10^4$ s.

Fig. 3 correspond to the lowest damping effectively measured in the experiment, $\gamma = 2/\tau = (1.68 \pm 0.02) \times 10^{-4}$ s^{-1}. Note that it is common in literature to report the dissipation in terms of a linewidth in Hz [14], which in our case is given by $\gamma/2\pi = (26.7 \pm 0.4)$ μHz.

In Fig. 4 we report the linewidth as a function of the pressure for the z-mode. The uncertainty is dominated by the error in the determination of pressure. We observe approximately a linear dependence on P, as predicted by standard gas damping models [36]. We note that the correction for the thermomolecular effect is accurate only in the low pressure limit but breaks down at higher pressure [34]. We take into account a possible deviation from linearity in the data by adding a quadratic term in the fitting function. The second order polynomial fit is shown in Fig. 4 together with the 90% confidence intervals. The linear term is (2.1 ± 0.1) Hz/mbar and can be directly compared with the gas damping prediction, given by [36]:

$$\gamma/2\pi = \frac{1}{\pi}\left(1 + \frac{8}{\pi}\right)\frac{P}{\varrho R v_{\rm th}} \tag{24}$$

where $v_{\rm th} = \sqrt{8k_BT/\pi m_g}$ is the mean thermal velocity of the gas and m_g is the molecular mass of helium. By inserting the numerical values we obtain $\gamma/(2\pi P) = 1.9$ Hz/mbar, in fair agreement with the experimental value. From the confidence intervals we infer a linewidth at zero pressure $\gamma_0/2\pi < 9$ μHz at 90% confidence level. We will

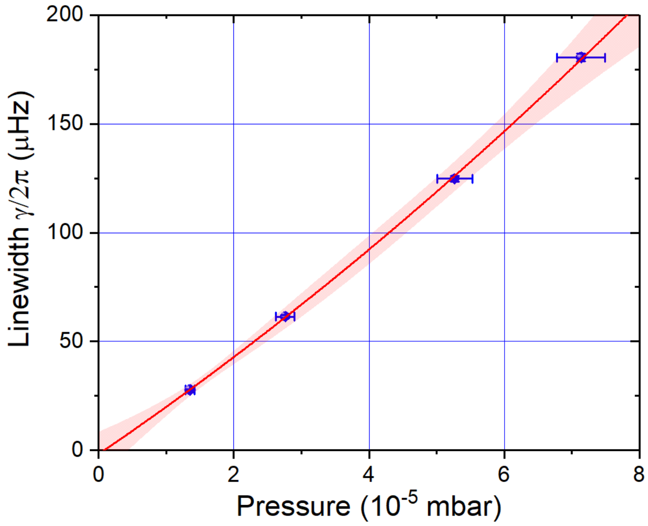

FIG. 4: Linewidth as a function of the pressure for the z-mode. A second order polynomial fit is shown, together with the 90 % confidence bands.

use this value as an upper limit on a possible dissipation arising from collapse models.

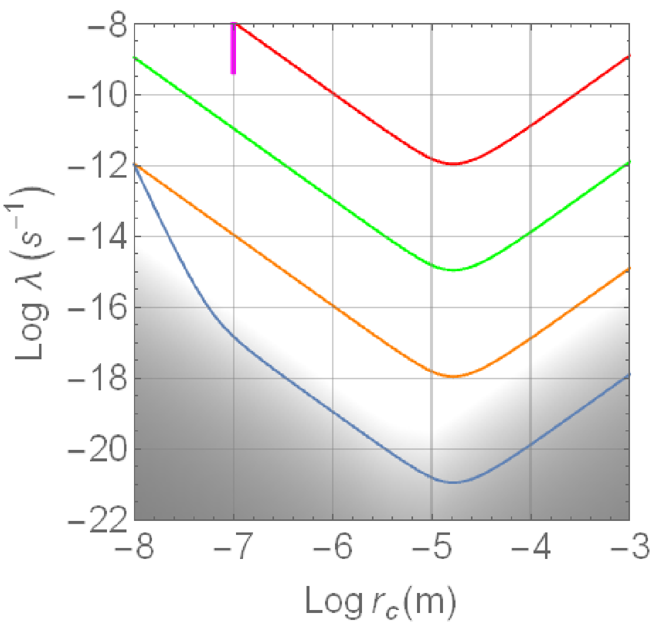

FIG. 5: Exclusion plot for the dCSL model in the $\lambda - r_c$ plane. The solid curves correspond, from top to bottom, to $T_c = 1$ K (red), $T_c = 10^{-3}$ K (green), $T_c = 10^{-6}$ K (orange), $T_c = 10^{-9}$ K (blue). The gray region is conventionally considered unnatural for the CSL model, as it would not guarantee an effective collapse of macroscopic quantum superpositions [31]. The vertical bar represents the enhanced values for λ at $r_c = 10^{-7}$ m proposed by Adler [29].

IV. DISCUSSION

A. The dCSL model

Our experimental data can be used to exclude the regions of the dCSL parameter space which predict a dissipation larger than the one measured in the experiment. Fig. 5 shows a family of curves in the $\lambda - r_c$ plane, each one corresponding to a fixed temperature T_c. The region above each curve is experimentally excluded by our experiment at 90 % confidence level. The gray region of parameter space is conventionally considered unnatural for the CSL model, as parameters well inside this region would not guarantee an effective collapse of macroscopic superpositions [31]. In other words the CSL model would no more accomplish its original scope. For $r_c = 10^{-7}$ m the gray region is equivalent to the initial value for λ proposed by Ghirardi *et al.* [2]. The vertical bar represents the enhanced values for λ proposed by Adler [29].

Clearly, our approach is particularly sensitive to low values of T_c, as these imply large values of dissipation. For $T_c \approx 10^{-9}$ K, the blue curve in Fig. 5, almost the entire natural parameter space of CSL is excluded. We also note a new feature on the left side of the $T_c \approx 10^{-9}$ K curve, with the slope which becomes much steeper, from a $\sim r_c^{-2}$ to a $\sim r_c^{-6}$ dependence. This corresponds to the transition from weak dissipation $\chi < 1$ to strong dissipation $\chi > 1$. Our results can be compared with a similar experiment performed with a nanoparticle in a Paul trap [14]. In particular, our bounds are more stringent for $r_c > 2 \times 10^{-7}$ m. If we compare our bounds on dCSL, based solely on dissipation, to the bounds on standard CSL inferred from noise measurements [19–22], we see that dissipation-based tests set stronger bounds than noise-based tests for $T_c < 10^{-2}$ K. We also notice that for $T_c < 10^{-2}$ K our experiments is substantially excluding the enhanced values for λ proposed by Adler.

B. The dDP model

For the dDP model, using for m_a in Eqs. (10) and (13) the mean nuclear mass, we find that our experiment does not provide any exclusion in the uniform matter limit Eq. (11). In the granular matter limit Eq. (14), it formally provides an exclusion region, but this corresponds to unphysical parameters $R_0 < 10^{-23}$ m. In fact, the Diósi-Penrose model is nonrelativistic, and this assumption breaks down for $R_0 \ll 10^{-15}$ m. Furthermore, in [13] it has been pointed out that already for $R_0 = 10^{-15}$ m a dissipative extension of the DP model would lead to instability of nuclear matter.

However, we find a significant exclusion by making a different choice for the reference mass m_a which appears in the expressions of $\chi_{\rm DP}$ and $\gamma_{\rm DP}$. Specifically, we can take as elementary entity for the dDP mechanism a sphere of radius $R_0' = R_0\,(1 + \chi_{\rm DP})$, i.e. $m_a = \frac{4\pi}{3}\varrho R_0'^3$. This choice is motivated by the fact, apparent from

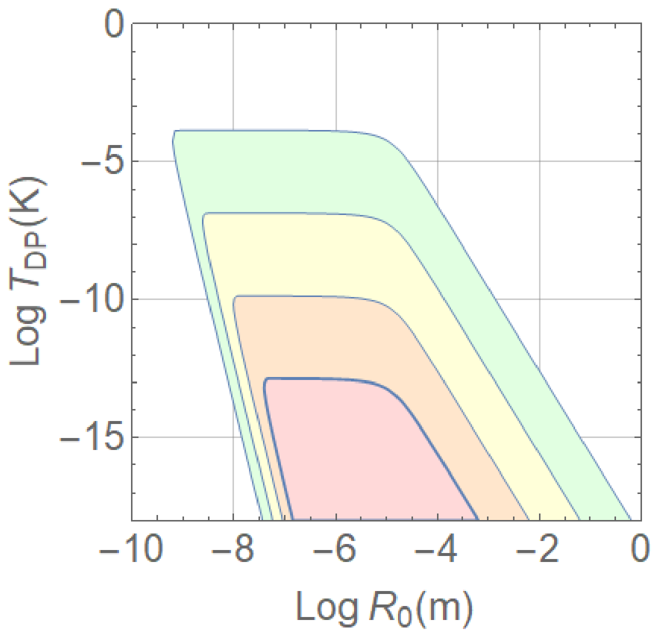

FIG. 6: Exclusion plot for the dDP model in the $T_{\rm DP} - R_0$ plane, by assuming $m_a = 4\pi/3\varrho R_0'^3$. The inner light red region is excluded by our experiment. The outer regions (orange, yellow, green) would be excluded by a reduction of the experimental dissipation rate by a factor $10^3, 10^6, 10^9$ respectively. The dDP model with $T_{\rm DP} = 1$ K would predict a dissipation rate 10^{13} times smaller than the observed one. The cut-off at $R_0 \approx 10^{-5}$ m is determined by the size of our particle.

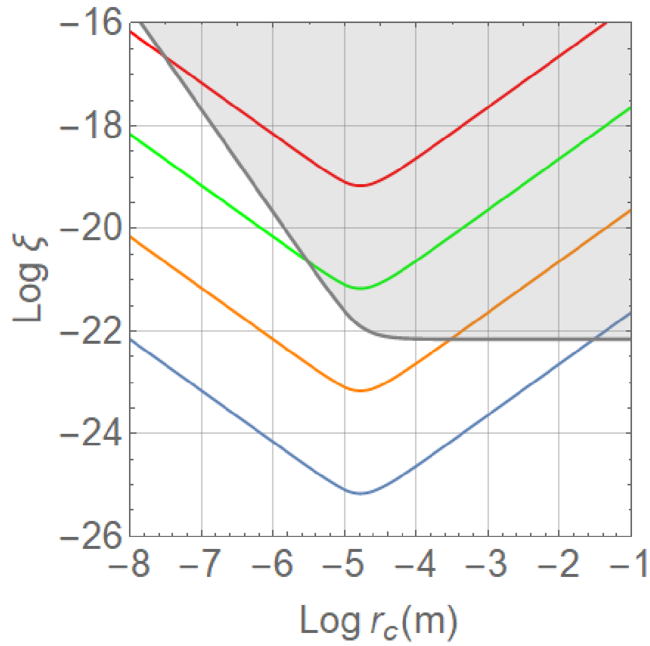

FIG. 7: Exclusion plot for the CGF model in the $r_c - \xi$ plane, where r_c is the correlation length and ξ is the magnitude of the complex fluctuations of the metric. The solid curves correspond, from top to bottom, to different correlation rate $\lambda = 10^{16}, 10^{14}, 10^{12}, 10^{10}$ Hz. The regions above the curve is excluded by the experiment. The thick gray curve correspond to the choice $\lambda = c/r_c$, and under this condition the gray region is excluded by the experiment.

Eq. (11), that the collapse mechanism is coherent within a sphere of radius R_0', that is $\eta_{\rm DP} \propto m^2$, while it scales linearly with the mass for $R > R_0'$. In other words, an object smaller than R_0' behaves as a single particle of mass m, meaning that the physics of the DP collapse mechanism is suppressed below the R_0' scale. Under this assumption, the excluded region in the $T_{\rm DP} - R_0$ parameter space, that is the region where the predicted dissipation is larger than the observed dissipation, is shown in Fig. (6). We note that the excluded region extends up to a temperature $T \approx 10^{-13}$ K. A given reduction of the measured dissipation rate γ would shift the bound up by the same factor. Therefore, we are roughly 13 orders of magnitude off from excluding the dDP model with $T_{\rm DP} = 1$ K. The upper bound on $T_{\rm DP}$ does not depend on the size of the object R. For larger R and same γ we would however observe a shift of the high R_0 cutoff, which is located at $R_0 \approx R$.

C. The CGF model

Fig. 7 shows the exclusion plot for the CGF mode in the (r_c, ξ) plane, where r_c is spatial correlation length and ξ is the magnitude of the complex gravity fluctuation. Different curves are plotted corresponding to different correlation times. A physical insight is provided by the thick blue curve, which is obtained by Eq. (21), i.e. by assuming that temporal and spatial correlations are related by c. This is suggested by the fact that the gravitational field propagates at speed of light [16]. The gray region is then excluded by our experiment. Interestingly, the order of magnitude of the probed region, down to 10^{-22} is comparable with the typical amplitude of the metric represented by astrophysical gravitational waves. It should be stressed that the fluctuations of the metric probed by our experiment have a nature quite different from gravitational waves: they are complex, and the correlation time is very short.

V. CONCLUSION

We have set new improved bounds on dissipative collapse models, based on measuring ultralow dissipation in a low frequency levitated micromagnet. Our data are essentially ruling out the dCSL model for collapse field temperatures of 10^{-9} K or lower. For the dDP model the exclusion is much weaker. By setting m_a as the mass of a sphere of radius R_0', we exclude field temperature $T_{\rm DP} < 10^{-13}$ K. We have also tested the magnitude of complex metric fluctuations suggested by the CGF model, and in particular we have set for the first time a bound on the imaginary part of the correlator of such fluctuations, directly related to dissipation. We have probed fluctuations of the metric with amplitude down to 10^{-22}.

Acknowledgments

A.V., C.T., G.G. and H.U. acknowledge financial support from the EU H2020 FET project TEQ (Grant No. 766900), the Leverhulme Trust (RPG-2016-046), the COST Action QTSpace (CA15220) and the Foundational Questions Institute (FQXi). M.T. acknowledges financial support from EPSRC (grant N. EP/N031105/1).

Appendix A: Calculational details for the granular limit (lattice model)

The amplification factor for spherical particles in the regime of tiny motional displacements, both for the CSL and DP models, has been discussed in detail in Ref. [37]. The dCSL and dDP models in the regime of tiny displacements have been discussed in Refs. [15] and [14].

The amplification factor can be well understood in terms of Adler's formula or within the homogeneous-body approximation, but the most refined modelling is based on a lattice model (for a comparison see [31]). Here we discuss the extension of the the latter [37] to the dissipative CSL and DP models – we will see that most of the analysis carries over to the dissipative variants. In particular, we focus on the regime where the effective localization lengths, $r_c' = r_c(1+\chi)$ and $R_0' = R_0(1+\chi_{\text{DP}})$, are smaller than the lattice constant a; we expect a linear scaling of the amplification parameter η or η_{DP} with the mass of the system as expected from Adler's formula. The other interesting regimes of the dissipative models for spherical particles have been reported in [14].

We consider the mass density of a spherical body:

$$\varrho(\boldsymbol{r}) = m_a \sum \delta(x - an_x)\delta(y - an_y)\delta(z - an_z)$$

where a is the lattice number, the sum is over the values $n_x^2 + n_y^2 + n_z^2 \leq n_{\text{max}}^2$, an_{max} is the radius of the body, and m_a is the mass of a unit cell. The Fourier transform of the mass density is given by

$$\tilde{\varrho}(\boldsymbol{q}) = \int d\boldsymbol{r}\,\varrho(\boldsymbol{r}) e^{i\frac{\boldsymbol{q}\cdot\boldsymbol{r}}{\hbar}}. \tag{A1}$$

For later convenience we evaluate

$$|\tilde{\varrho}(\boldsymbol{q})|^2 = m_a^2 \sum\sum e^{i\frac{aq_x \Delta n_x}{\hbar}} e^{i\frac{aq_y \Delta n_y}{\hbar}} e^{i\frac{aq_z \Delta n_z}{\hbar}} \tag{A2}$$

where $\Delta n_j = n_j - l_j$, and the double sum is over the values $n_x^2 + n_y^2 + n_z^2 \leq n_{\text{max}}^2$ and $l_x^2 + l_y^2 + l_z^2 \leq n_{\text{max}}^2$.

The dCSL case

We start from

$$\eta = \left[\frac{\nu^2}{(2\pi\hbar)^3}\frac{1}{\hbar^2}\right] \int d\boldsymbol{q} |\tilde{\varrho}(\boldsymbol{q})|^2 e^{-\frac{r_c^2(1+\chi)^2\boldsymbol{q}^2}{\hbar^2}} q_x^2, \tag{A3}$$

where

$$\nu^2 = \frac{\lambda r_c^3 (4\pi)^{3/2}}{m_0^2}. \tag{A4}$$

Using Eq. (A2) we readily find:

$$\begin{aligned}\eta =& \frac{\nu^2}{(2\pi)^3}\frac{\pi^{\frac{3}{2}} m_a^2}{4r_c'^7} \times \\ & \sum\sum \left(2r_c'^2 - a^2\Delta n_x^2\right) e^{-\frac{a^2\left(\Delta n_x^2 + \Delta n_y^2 + \Delta n_z^2\right)}{4r_c'^2}}.\end{aligned} \tag{A5}$$

We now assume $a \gg 4r_c'$ such that only the terms satisfiying $\Delta n_x^2 = \Delta n_y^2 = \Delta n_z^2 = 0$ contribute; the contribution from a single sum is m/m_a. This immediately gives

$$\eta = \frac{\nu^2 m_a m}{16\pi^{3/2} r_c'^5}. \tag{A6}$$

We now use Eq. (A4) to find

$$\eta = \frac{\lambda}{2(1+\chi)^5 r_c^2}\frac{m_a m}{m_0^2}. \tag{A7}$$

The dDP case

We start from

$$\eta_{\text{DP}} = \left[\frac{G}{2\pi^2\hbar^2}\frac{1}{\hbar^2}\right] \int d\boldsymbol{q} |\tilde{\varrho}(\boldsymbol{q})|^2 e^{-\frac{R_0^2(1+\chi_{\text{DP}})^2\boldsymbol{q}^2}{\hbar^2}} \frac{q_x^2}{\boldsymbol{q}^2}. \tag{A8}$$

We insert Eq. (A2) and, similarly as for dCSL, assume $a \gg 4(1+\chi_{\text{DP}})R_0$ such that only the terms satisfiying $\Delta n_x^2 = \Delta n_y^2 = \Delta n_z^2 = 0$ contribute. We then find

$$\eta_{\text{DP}} = \frac{G}{6\hbar\sqrt{\pi}(1+\chi_{\text{DP}})^3 R_0^3} m_a m. \tag{A9}$$

We obtain the same result from [37] with the formal replacement $R_0 \to R_0' = (1+\chi_{\text{DP}})R_0$.

[1] G.C. Ghirardi, A. Rimini, and T. Weber, Unified dynamics for microscopic and macroscopic systems, Phys. Rev. D **34**, 470 (1986).

[2] G.C. Ghirardi, P. Pearle, and A. Rimini, Markov processes in Hilbert space and continuous spontaneous localization of systems of identical particles, Phys. Rev. A **42**, 78 (1990).

[3] L. Diósi, Models for universal reduction of macroscopic quantum fluctuations, Phys. Rev. A **40**, 1165 (1989).

[4] R. Penrose, On Gravity's role in Quantum State Reduction, Gen. Relativ. Gravit. **28**, 581 (1996).

[5] A. Bassi and G.C. Ghirardi, Dynamical reduction models, Phys. Rep. **379**, 257 (2003).

[6] A. Bassi, K. Lochan, S. Satin, T. P. Singh, and H. Ulbricht, Models of wave-function collapse, underlying theories, and experimental tests, Rev. Mod. Phys. **85**, 471 (2013).

[7] D. Carney, P.C.E. Stamp, J.M. Taylor, Tabletop experiments for quantum gravity: a user's manual, Class. Quantum Grav. **36** 034001 (2019).

[8] S.L. Adler, Gravitation and the noise needed in objective reduction models, in *Quantum Nonlocality and Reality: 50 Years of Bells Theorem*, ed. M. Bell and S. Gao (Cambridge University Press, Cambridge, UK).

[9] A. Bassi, A. Grossardt, and H. Ulbricht, Gravitational Decoherence, Class. Quantum Grav. **34**, 193002 (2017).

[10] T. Josset, A. Perez, D. Sudarsky, Dark Energy from Violation of Energy Conservation, Phys. Rev. Lett. **118**, 021102 (2017).

[11] A. Tilloy, and L. Diósi, Sourcing semiclassical gravity from spontaneously localized quantum matter, Phys. Rev. D **93**, 024026 (2016).

[12] A. Smirne and A. Bassi, Dissipative Continuous Spontaneous Localization (CSL) model, Sci. Rep. **5**, 12518 (2015).

[13] M. Bahrami, A. Smirne and A. Bassi, Role of gravity in the collapse of a wave function: A probe into the Disi-Penrose model, Phys. Rev A **90**, 062105 (2014).

[14] A. Pontin, N.P. Bullier, M. Toroš, and P.F. Barker, An ultra-narrow line width levitated nano-oscillator for testing dissipative wavefunction collapse, Phys. Rev. Research **2**, 023349 (2020).

[15] J. Nobakht, M. Carlesso, S. Donadi, M. Paternostro, and A. Bassi, Unitary unraveling for the dissipative continuous spontaneous localization model: Application to optomechanical experiments, Phys. Rev. A **98** 042109 (2018).

[16] G. Gasbarri, M. Toroš, S. Donadi, and A. Bassi, Gravity induced wave function collapse, Phys. Rev. D **96**, 104013 (2017).

[17] M. Toroš, G. Gasbarri, and A. Bassi, Colored and dissipative continuous spontaneous localization model and bounds from matter-wave interferometry, Phys. Lett. A **381**, 3921 (2017).

[18] Y.Y. Fein, P. Geyer, P. Zwick, F. Kiałka, S. Pedalino, M. Mayor, S. Gerlich, and M. Arndt, Quantum superposition of molecules beyond 25 kDa, Nat. Phys. **15**, 1242 (2019).

[19] A. Vinante, M. Bahrami, A. Bassi, O. Usenko, G. Wijts, and T.H. Oosterkamp, Upper Bounds on Spontaneous Wave-Function Collapse Models Using Millikelvin-Cooled Nanocantilevers, Phys. Rev. Lett. **116**, 090402 (2016).

[20] A. Vinante, R. Mezzena, P. Falferi, M. Carlesso, and A. Bassi, Improved Noninterferometric Test of Collapse Models Using Ultracold Cantilevers, Phys. Rev. Lett. **119**, 110401 (2017).

[21] A. Vinante, M. Carlesso, A. Bassi, A. Chiasera, S. Varas, P. Falferi, B. Margesin, R. Mezzena, and H. Ulbricht, Narrowing the parameter space of collapse models with ultracold layered force sensors, arXiv:2002.09782.

[22] M. Carlesso, A. Bassi, P. Falferi, and A. Vinante, Experimental bounds on collapse models from gravitational wave detectors, Phys. Rev. D **94**, 124036 (2016).

[23] B. Helou, B. Slagmolen, D.E. McClelland, and Y. Chen, LISA pathfinder appreciably constrains collapse models, Phys. Rev. D **95**, 084054 (2017).

[24] D. Zheng *et al.*, Room temperature test of wave-function collapse using a levitated micro-oscillator, Phys. Rev. Research **2**, 013057 (2020).

[25] M. Bilardello, S. Donadi, A. Vinante and A. Bassi, Bounds on collapse models from cold-atom experiments, Phys. Rev. A **462**, 764 (2016).

[26] K. Piscicchia, A. Bassi ,C. Curceanu, R. Del Grande, S. Donadi, B.C. Hiesmayr, and A. Pichler, CSL Collapse Model Mapped with the Spontaneous Radiation, Entropy **19**, 319 (2017).

[27] S.L. Adler and A. Vinante, Bulk heating effects as tests for collapse models, Phys. Rev. A **97**, 052119 (2018).

[28] This assumption is usually valid in the CSL model, because too small r_c would lead to appreciable effects in microscopic systems. However, for sake of completeness, we report in Appendix the derivation of the parameter η for the case $r_c \ll a$.

[29] S.L. Adler, Lower and upper bounds on CSL parameters from latent image formation and IGM heating, J. Phys. A **40**, 2935 (2007).

[30] G.C. Ghirardi, R. Grassi, and A. Rimini, Continuous-spontaneous-reduction model involving gravity, Phys. Rev. A **42**, 1057 (1990).

[31] M. Toroš and A. Bassi, Bounds on quantum collapse models from matter-wave interferometry: calculational details, J. Phys. A **51**, 115302 (2018).

[32] M. Blencowe, Effective Field Theory Approach to Gravitationally Induced Decoherence, Phys. Rev. Lett. **111**, 021302 (2013).

[33] K. Krasnov, Gr uniqueness and deformations, Journ. High En. Phys. **2015**, 37 (2015).

[34] A. Vinante, P. Falferi, G. Gasbarri, A. Setter, C. Timberlake and H. Ulbricht, Ultralow Mechanical Damping with Meissner-Levitated Ferromagnetic Microparticles, Phys. Rev. Applied **13**, 064027 (2020).

[35] T.R. Roberts and S.G. Sydoriak, Thermomolecular Pressure Ratios for He^3 and He^4, Phys. Rev. **102**, 304 (1956).

[36] P.S. Epstein, On resistance experienced by spheres in their motion through gases, Phys. Rev. **23**, 710 (1924).

[37] S. Nimmrichter, K. Hornberger, and K. Hammerer, Optomechanical Sensing of Spontaneous Wave-Function Collapse, Phys. Rev. Lett. **113**, 020405 (2014).